11th International Symposium on Magnetic Bearings
August 26-29, Nara, Japan

AXIAL MAGNETIC BEARING DEVELOPMENT FOR THE BIVACOR ROTARY BIVAD/TAH

Nobuyuki Kurita
Miyakonojo National College of Technology, Miyakonojo, Miyazaki 885-8567, Japan
nkurita@cc.miyakonojo-nct.ac.jp

Daniel L Timms
The prince Charles Hospital, Brisbane, QLD, 4032, Australia
daniel_timms@health.qld.gov.au

Nicholas Greatrex
Queensland University of Technology, Brisbane, QLD, 4000, Australia
n.greatrex@student.qut.edu.au

Toru Maszawa
Ibaraki University, Hitachi, Ibaraki 316-8511, Japan
masuzawa@mx.ibaraki.ac.jp

ABSTRACT
A third generation rotary BiVAD/TAH is under development to treat end stage bi-ventricular heart failure. The device includes a set of left and right vanes positioned on a rotating hub to form a double-sided centrifugal impeller. Since the LVAD and RVAD impeller vanes are inherently coupled to the common rotation hub, changes in speed will alter the outflow of the left and right VAD's. However, to account for required changes in instantaneous left/right outflow, the magnetic bearing system can displace the impeller axially within the pump cavity. This action simultaneously alters the efficiency of each semi-open impeller vane set in an inverse relationship.

To develop the rotary BiVAD, a magnetic levitated motor bearing is designed and fabricated. The test rig consists of magnetic bearing, rotor and motor. The axial magnetic bearing, include permanent magnets for bias flux is constructed from U-shaped magnetic bearing. The motor was constructed from 6 poles of which concentrated copper coils were wound. The motor stator was electromagnetically coupled to the rotor via 4 permanent magnets attached to an iron core on the rotor.

To confirm the performance of fabricated test rig, static and dynamic characteristics are measured. The power consumption was 15 W, while predicted power consumption was 10 W. However the step response demonstrated good control performance and successful levitated rotation about 3750 rpm was achieved.

The experimental results were discussed for to produce a miniature implantable device suitable for chronic animal implantation.

INTRODUCTION
The incidence of chronic or congestive heart failure (CHF) is increasing as the general population ages. As many as 550,000 new cases are diagnosed in the United State each year, however less than one percent of patients receive a heart transplant [1]. Therefore, the use of mechanical device therapy to treat cardiovascular disease is increasing while the number of donor organs remains limited.

Devices can be used to bridge a patient to heart transplant, to recovery, or indeed as a destination alternative. The latter support strategy requires a device with increased mechanical durability/lifetime.

Mechanical durability is dependent on the functionality of the device, in particular type of bearings implemented. First generation pulsatile devices necessitate contacting components, which limits their predicted mechanical lifetime below three years. The reduced size of second generation non-pulsatile rotary impeller devices has accelerated them to the forefront of current VAD research. However, initial techniques for impeller support also imposed significant limitations on device lifetime, as they required a shaft, seals and bearings [2, 3]. Subsequent improvements resulted in second generation devices that rely on blood immersed pivot support [4, 5]; however predicted service life is still below five years. Several techniques have since been developed to improve device lifetime, ranging from complete magnetic suspension [6-8], to passive hydrodynamic suspension [9, 10]. These third generation devices eliminate contact wear and reduce the number of moving components, potentially increasing device lifetime to beyond ten years.

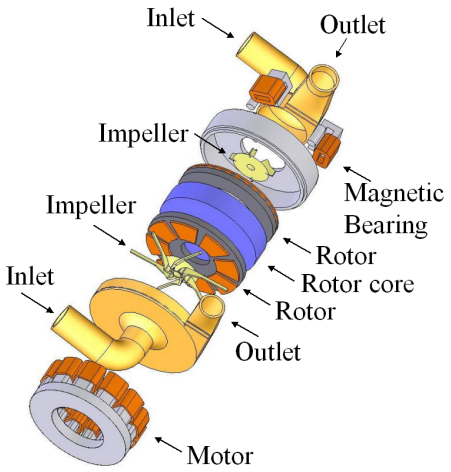

FIGURE 1: A schematic of the BiVACOR device

As opposed to hydrodynamic suspension, magnetic bearing technology boasts non-contact impeller suspension with larger clearance gap [11]. This eliminates any point-to-point contact with reduced shear stress, which may improve the hemolytic performance of the pump. However, the power consumed by the device may increase, and is ideally maintained below 10 W to reduce the potential for heat damage.

Hoshi et al. provides a comprehensive review of non-contact magnetic bearings for rotary blood pumps [12]. The review details the operation of a number of commercial devices, as well as research devices that implement magnetic bearing technology. For example, the Duraheart (Terumo, Ann Arbor, MI, USA) uses an axial magnetic bearing with a permanent magnet coupling motor [13]. Heartmate III (Thoratec, Woburn, MA, USA) uses a combined radial self-bearing motor [14], while the Levacor (formerly Heartquest, World-heart, Ottawa, ON, Canada) uses an axial magnetic bearing and electromagnetically coupled motor [15].

All of the devices mentioned provide left ventricular assistance (LVAD). However, a significant number of patients also require a device for right ventricular assistance (RVAD). The incidence of bi-ventricular failure is not always initially apparent in heart failure patients, and right ventricular heart failure may develop in up to 40% of patients receiving LVAD assistance [16-20]. The most successful BiVAD system used in clinical practice is the extracorporeal connection of two Thoratec devices [21]. However, smaller rotary systems have been proposed which make use of two implanted rotary pumps, such as the combined Coraide+ Dexaide [17] and two Gyro pumps [18].

All of these bi-ventricular assist systems require the use of two devices, which increases implantation size as well as the cost of the therapy. Therefore, the authors are focused on developing a single rotary BiVAD suitably sized for implantation.

The third generation BiVACOR bi-ventricular assist device aims to treat end stage bi-ventricular heart failure with a single rotary device. The device, shown in FIGURE 1, includes a set of left and right vanes positioned on rotating hub to form a double-sided centrifugal impeller. Active impeller suspension is achieved with an axial magnetic bearing and rotation via an electromagnetically coupled motor. Since the LVAD and RVAD impeller vanes are inherently coupled to the common rotation hub, changes in speed will alter the outflow of the left and right VAD's. However, to account for required changes in instantaneous left/right outflow, the magnetic bearing system can displace the impeller axially within the pump cavity. This action simultaneously alters the efficiency of each semi-open impeller vane set in an inverse relationship. I.e. a movement toward the left cavity will increase LVAD outflow while reducing RVAD outflow, and vice-versa.

The objective of this research was to therefore investigate the dynamic behavior of the magnetic suspension system and determine the range of possible impeller axial movement while maintaining suitable power consumption.

MATERIAL AND METHODS

Magnetic System Identification-Hydraulic forces

When attempting to design a magnetic bearing, the system and thus operating parameters for which it must operate should be determined. In the case of levitated impeller for a VAD application, the magnetic levitation and motor system must be able to counteract disturbing hydraulic forces cased by impeller hydraulic operation and natural cardiac interaction, as well as to produce sufficient torque for energy transferal to the blood.

To this end, a motor-shaft driven prototype device complete with force transducer (50M31, Jr3 Inc. Woodland, CA, USA) was inserted into a mock circulation loop [22] to measure and therefore predict the axial hydraulic force encountered by the impeller in pulsatile and non-pulsatile circulatory environments. The technique [23] can be used to determine the expected axial loads when operating the device in a BiVAD/TAH mode. Furthermore, the torque requirements of the device should be calculated prior to design. Considering the VAD requires and output power of approx 1.33 W to provide normal hemodynamics to the systemic and pulmonary system, and assuming a device hydraulic efficiency of 30%, the motor must generate 4.43 W. With an assumed rotational speed for this condition of 2000 rpm, the torque requirement of the motor is 0.021 Nm. However, higher torque values up to 0.04 Nm may be needed for elevated hemodynamic requirements.

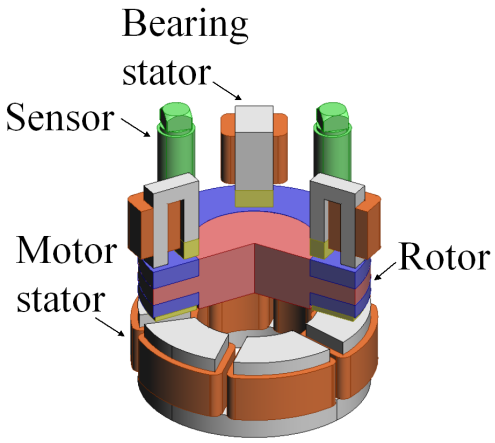

FIGURE 2: A schematic of the magnetic motor-bearing system

Magnetic Bearing Design

The BiVACOR Bi-VAD/TAH incorporates an electromagnetic motor and active axial magnetic bearing to respectively provide rotational torque and contact free impeller suspension. A diagram of the magnetic system is shown in FIGURE 2. The experimental setup consists of magnetic bearing, rotor and motor. The axial magnetic bearing is constructed from three evenly spaced (120°) U-shaped bearing stators. 276 turns of ϕ0.4 mm copper wire were wound about the outside foot of each stator to produce flux directed towards an iron core attached to the rotor. A custom NdFeB permanent magnet was attached to the inner foot of each core to provide bias flux to the magnetic flux path.

The slotted axial flux motor was constructed from 6 poles of which concentrated copper coils were wound. The motor stator was electromagnetically coupled to the rotor via 4 permanent magnets attached to an iron core on the rotor.

Feedback control of the rotor's axial position was achieved in response to rotor displacement detected by three eddy current sensors (U5B, Lion Precision, MN, USA). These displacement measurements were the feedback parameters used by the PD controller to stabilize the system. The controller was developed and implemented on the dSPACE data acquisition system (DS1104, dSPACE, MI, USA). Control gains were output to a custom power amplifier, which generated the required current in the corresponding coil to alter the flux density in the magnetic gap and thus attractive force to maintain rotor levitation. Similarly, the open loop motor controller generates the three phases current for the motor coils to provide synchronous rotation.

TABLE 1: Parameters of the equations

B_R	The peak flux density of the motor
B_S	The peak flux density of the stator
M	The pole pair number of the motor
ω	The rotating speed of the rotor
ϕ	The phase difference
r_1	The inner radius of the rotor
r_2	The outer radius of the rotor
z	The equivalent distance of the air gap
μ_0	The permeability of vacuum

Magnetic Theory. Axial attractive force f_z and the motor torque τ_z produced form the magnetic motor and bearing system can be derived from Eq. (1) and Eq. (2).

$$f_z = \frac{(r_2^{\,2} - r_1^{\,2})\pi}{4\mu_0}\left[B_R^{\,2} + 2B_R B_S \cos\phi + B_S^{\,2}\right] \quad (1)$$

$$\tau_z = \frac{zM(r_2^{\,2} - r_1^{\,2})\pi}{2\mu_0} B_R B_S \sin M\phi \quad (2)$$

Given our identified axial force and torque design criteria, B_r and B_s are calculated. The stator (B_s) and the permanent magnet flux of the rotor (B_r) are assumed to follow a cosine waveform magnetic flux density and as described by Eq. (3) and Eq. (4)

$$B_s(\theta, t) = B_S \cos(\omega t - M\theta) \quad (3)$$

$$B_r(\theta, t) = B_R \cos(\omega t - M\theta - \phi) \quad (4)$$

The number of turns in the coils and the geometric parameters of the permanent magnets can then be determined to produce this calculated flux.

The parameters used in each equation are listed in TABLE 1. To simplify calculation, we assume the magnetic properties of the material to be homogeneous and its reluctance can be ignored.

From this theory, changing the magnitude of magnetic flux of the motor stator B_S and the attractive force by the magnetic bearing can control the axial displacement of the rotor. The motor torque is also controlled changing the phase different ϕ.

The operation principle of the tilt control by the magnetic bearing is shown in FIGURE 3. The constant bias flux is produced by the permanent magnets. When

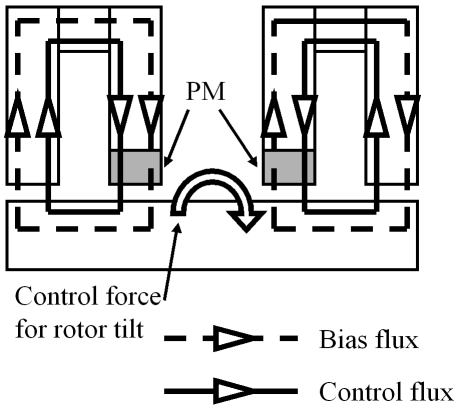

FIGURE 3: Operation principle of the tilt control by the magnetic bearing

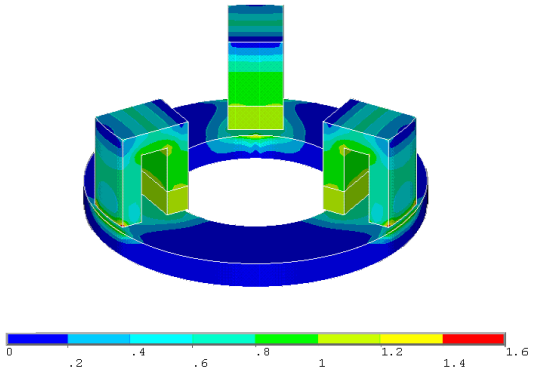

FIGURE 4: The result of 3D FEM analysis

the motor tilt, the flux in the side that the rotor approaches is decreased and the flux in the other side is increased by the control flux with the electromagnet.

FEM Analysis and System Specifications. In order to refine the initial design development from the magnetic theory, the calculated parameters were input to ANSYS model of system to predict the force characteristics. The model refines design by including the influence of leakage flux. FEM analysis was carried out to obtain 15N of attractive force by the permanent magnets. The analytical result of flux density is shown in FIGURE 4. According to the analytical result detailed specifications of the axial motor bearing are provided in TABLE 2.

Static and Dynamic Characteristics

To confirm the practical force capacity of the magnetic motor-bearing system, a suitable test rig was developed. A shaft was introduced to support the rotor at precise distance from the magnetic bearing stators. The other end of the shaft was connected to the force transducer in

TABLE 2: Refined specifications of the axial motor-bearing

Bearing (S45C Iron)		
Stator height		21.5 mm
Coil turns (ϕ0.4)		276 turns/pole
PM flux density		N45
PM thickness		3 mm
Motor (S45C Iron)		
Stator height		10 mm
Coil turns (ϕ0.4)		180 mm
PM thickness		1 mm
Rotor (Disc: S45C, Core: POM)		
Outer diameter		ϕ49 mm
Inner diameter		ϕ27 mm
Thickness	(bearing side)	2 mm
	(motor side)	2 mm
	(core)	8 mm

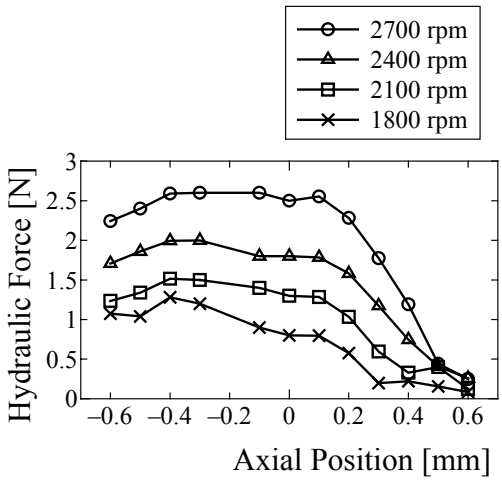

FIGURE 5: Hydraulic force encountered on the device impeller operated as a TAH in the circulation loop configured for total heart failure

order to record the attractive force produced by the bearing and motor stator for a current range of +/-3 A. Following these static experiments, three separate conditions were simulated to test the dynamic performance of the system. Test was initially conducted with a constant impeller position centralized in the pump cavity, and speed was increased from 0-3750 rpm while rotor axial stability was recorded. The speed was then held at a constant 0 rpm and 2500 rpm, while impeller axial stability was again recorded at various axial positions. Finally, the step response of the impeller to discrete changes in axial position was recorded to evaluate the performance of the controller.

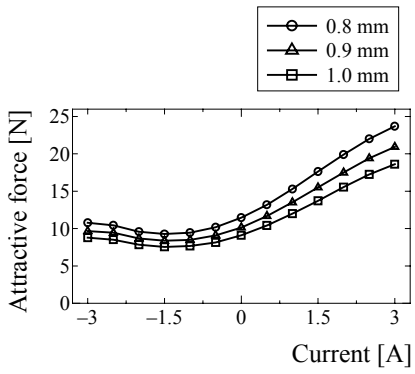

(a) Attractive force of the magnetic bearing

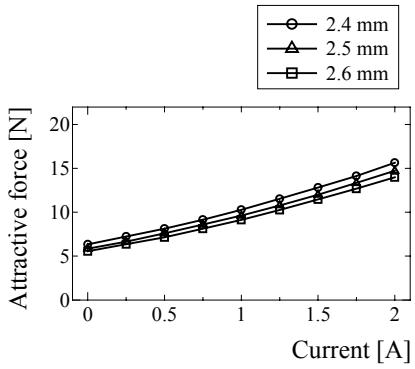

(b) Attractive force of the motor

FIGURE 6: Attractive force results from the magnetic bearing (a) and motor (b) for specified current range with various magnetic airgaps.

EXPERIMENTAL RESULTS

Mock Loop

Operating the shaft mounted BiVAD impeller while connected to the circulation loop replicating pulsatile bi-ventricular heart failure produced a maximum impulse force of 12 N. Removing heart pulsatility from the loop, and thus simulating total bi-ventricular heart failure, a maximum force of 3 N was produced. This force reduced as impeller position was altered to the extreme range of +/-0.6 mm from the central position (see FIGURE 5)

Force Measurement

Magnetic force measurements with varying axial airgaps and excitation current were recorded for the levitation system, with result for bearing and motor attraction displayed in FIGURE 6 (a) and FIGURE 6 (b).

The three bearing stators produced a combined force of 10 N at zero current and magnetic airgap of 0.9 mm

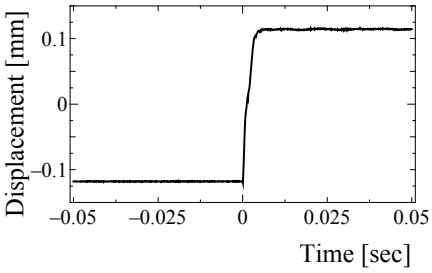

FIGURE 7: Step response of center of gravity

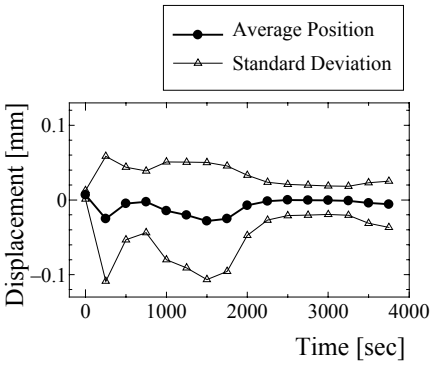

FIGURE 8: Constant central axial position with changing speed from 0 to 3750 rpm

which represents a central impeller position of 0 mm. A current stiffness of 3.6 N/A was produced for positive flowing current, however this reduced significantly with negative current, due to the inability for the active magnetic flux to efficiently cancel the permanent magnetic flux.

With an additional rotor weight of 1 N, the motor stator produced a balancing attractive force of 9 N at 2.5 mm airgap, with 1 A current. A constant 1 A bias current was considered essential to produce sufficient torque for rotation when required.

The current stiffness for positively flowing current at this position was 5 N/A. The attractive forces from the motor and bearing changed as the rotor deviated from the axial central position by +/-0.1 mm.

From the presented results, it is clear that the force generated flows a distinct nonlinear function when the current is varied through both bearing and motor coils. Additionally it can be seen that the force is a nonlinear function of displacement.

Levitation and Rotation

The subsequent assessment of the magnetic system demonstrated stable levitation and rotation. Energy consumption of the bearing and motor was measured when rotor was levitated without and with rotation.

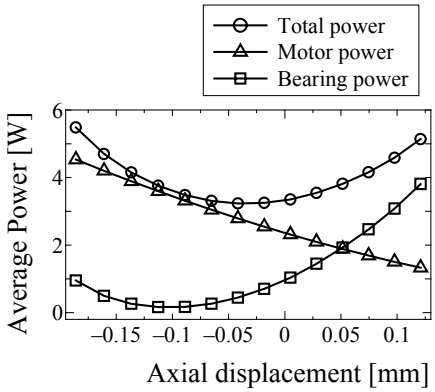

FIGURE 9 (a): Power consumption with axial displacement with no rotation

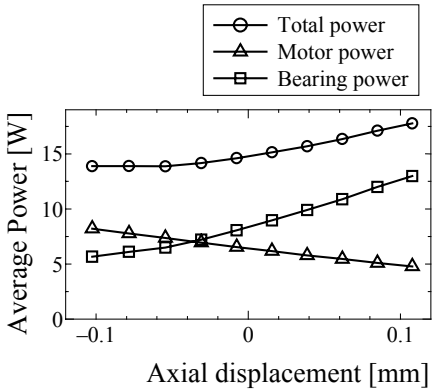

(b) 2500 rpm

FIGURE 9 (b): Power consumption with axial displacement with 2500 rpm

Levitation Characteristics. To confirm the control performance of the magnetic bearing, the step response was measured. The reference step signal was input to the displacement of the center of gravity and the average of the sensor signal was recorded when the rotational speed was 0 rpm. The result of the step response is shown in FIGURE 7. Rotor vibration was stable following a step of 0.2 mm, demonstrating good control performance.

Levitated Rotation Characteristics. A levitated rotation test was conducted to evaluate the performance of the system. Three-phase AC current was applied to the motor to rotate the rotor while its axial position was controlled to the center of the cavity. The result is shown in FIGURE 8. At speeds lower than 1800 rpm, the vibration of the rotor had a maximum amplitude of 0.11 mm. However, the vibration is reduced to +/-0.02 mm at 2500 rpm, which is the targeted rotating speed of

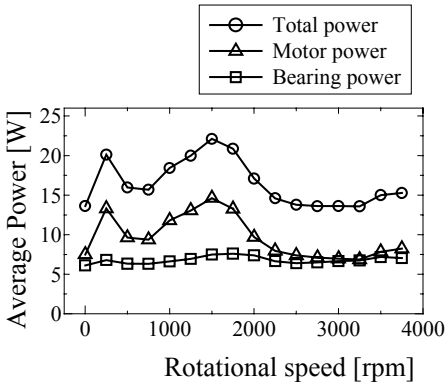

FIGURE 9 (c): Power consumption with changing rotor speed from 0 to 3750 rpm at constant 0 mm of axial displacement

the proposed magnetic motor bearing system for BiVAD application.

Power Consumption. Axial displacement of the rotor was possible; however, an increase in power consumption was observed when the rotor was moved from the central position. FIGURE 9 (a) shows the power consumption for axial displacement with no rotation. Bearing power was maximum when the rotor was closer to the motor stator (-ve direction), while motor power was maximum when the rotor was closest to the bearing stator (+ve direction). The total power consumption was below 6 W for an axial displacement of +/-0.15 mm. FIGURE 9 (b) shows the power consumption for axial displacement at rotation speed of the rotor was 2500 rpm. The changing behave of the power consumption was similar to the same test with rotation, however the DC offset of the motor current was increased to obtain 2500 rpm rotation speed. This caused the power consumption of the bearing also increase to counter the additional motor force generated by this offset. The total power consumption was below 18 W for an axial displacement of +/-0.15 mm and 14.5 W for 0 mm axial displacement. FIGURE 9 (c) shows the power consumption for changing speed of the rotor from 0 to 3750 rpm at constant 0 mm of axial displacement. The total power consumption was below 15 W for targeted BiVAD speed of 2500 rpm.

DISCUSSION

Magnetic levitation is a viable suspension technique for the impeller of an artificial heart to improve device lifetime and reduce blood damage.

To operate effectively, the magnetic bearing system is required to keep the impeller centered within pump clearances while providing actuation or rotational torque for all six coordinates (three translational x, y, z and

three moments θ_x, θ_y, θ_z). This may be achieved with a combination of passive and active forces. These systems utilize reluctance for Lorentz magnetic force to provide active radial (x, y), axial (z) or total (x, y, z, θ_x, θ_y, θ_z) suspension. For use in a centrifugal pump, an axial bearing improves performance due to the ability to incorporate more magnetic material in the unused axial surface area of the impeller [6].

Karassik and McGuire state that bearing power is usually only needed for magnetic excitation of disturbance forces [24]. Incorporating permanent magnets into the magnetic bearing system, while using active electromagnets for fine control, can reduce power consumption.

In the implantable blood pump application, the bearing must counter disturbing forces due to the hydraulic pressure developed within the pumping chamber. Precise determination of these load must be specified in order to complete the bearing design [25].

The results from the prototype connected to the mock circulation loop revealed a relatively large impulse force of 15 N in the BiVAD application. However, this force will decrease with blood damping of the suspended impeller. The magnetic suspension system must overcome this force by increasing the supply current to the active magnetic coils.

The theoretical magnetic flux required for sufficient force generation in the motor and bearing stators was then calculated using these hydraulic forces as design criteria. However, although these equations allow the initial geometric design of the magnetic components, it is well known that these equations overestimate the actual force production capacity of a magnetic system due to the lack of simulated flux path leakage and non-linear permeability of the iron core. Therefore, ANSYS finite element methods are frequently used to predict the force generation performance of the system.

Following simulation, the model must be validated with practical measurements. In this case, the prototype magnetic bearing could produce a 10 N force at a 0.9 mm airgap. This value was lower than the simulated value of 15 N. Practical measurements also conducted with the motor airgap of 2.5 mm when 1 A of current was supplied to the motor coils and the rotor weight was directed toward the motor stator. This static value of offset motor current was included to provide sufficient rotational torque to enable levitated rotation to the desired speed of 2500 rpm.

Constructing a test rig including a 0.9 mm airgap from the bearing and 2.5 mm airgap from the rotor resulted in the magnetic zero point residing within the +/-0.2 mm clearance gap between the rotor and pump cavity housing. The magnetic levitation system will be designed to operate around this point to minimize the power used to levitate to rotor under normal operating conditions.

Additional force measurements revealed that both the motor and bearing could produce sufficient balancing force when the impeller was move off the centralized position. For example, a movement of 0.1 mm toward the motor reduced the airgap to 2.4 mm and thus increased its attractive force to 10.3 N. This required the supply of +0.75 A to the bearing, now operating with an airgap of 1.0 mm, to produce a 11.3 N restoring force. Likewise, a movement of 0.1 mm toward the bearing required –0.5 A current supply to each bearing coil to partially cancel the PM flux and balance force.

All force results exhibited nonlinear force characteristics dependent on both current and displacement. To reduce the force generated by the permanent magnets, the coil current is reversed to cancel the bias flux. However, it can be seen that even at point of minimum force, a small force is still generated. This is due to the coil flux not completely canceling the permanent magnet flux due to significant leakage flux. This phenomenon was confirmed using finite element software. Further design iterations will seek to reduce this problem and allow for greater cancellation of the bias flux.

The performance of the levitation system was sufficient to maintain stable levitation and rotation at speeds required for BiVAD support. However, no load power consumption was recorded at approximately 15 W. This value is higher than the ideal power consumption of 10 W, and is attributed to the axial and radial vibration of the rotor during rotation. This is confirmed with the power consumption results of less than 5 W for +/-0.15 mm axial displacements at 0 rpm. The axial and radial vibration and thus power consumption may be reduced by conducting the levitated rotation tests with the rotor suspended in a viscous fluid. Furthermore, improvements to the levitation controller, by including non-linear parameters, may also improve performance.

CONCLUSION

An axial magnetic-motor rig was designed and constructed, and suspension characteristics of the system evaluated for use in an implantable BiVAD. Total magnetic bearing and motor power was below 16 W for an axial displacement of +/-0.15 mm and rotational speed of 2500 rpm. According to the step response, rotor vibration stabilized after step of 0.2 mm, which demonstrates good control performance. The rotor could maintain successful levitation up to 3750 rpm. Design optimization is underway to produce a miniature implantable device suitable for chronic animal implantation.

FUTURE WORKS

The energy consumption with levitated rotation was higher than the design point of 10 W. Therefore, the next iteration of the experimental setup is under fabrication to both reduce energy consumption and improve levitated rotation performance. The current magnetic components are constructed from mild steel, which typically has poor magnetic properties. Future design iterations will incorporate more appropriate materials, such as silicon steel and lamination techniques. Furthermore, the eventual combination of magnetic system with the radial journal bearing, operated in viscous fluid should improve radial stability and reduce vibration. Finally, the performance of the system will be assessed in simulated clinical conditions using a mock circulation loop, prior to implantation and evaluation in a chronic animal model.

ACKNOWLEDGEMENT

QUT workshop and MNCT workshop for fabrication of the experimental setup, and Eisuke Sasaki at Ibaraki University for assistance with the 3D simulation.

References

1. Wayne, R, et al., Heart Disease and Stroke Statistics, 2007 Update. Circulation, 2007. 115: p. 69-171.
2. Wampler, R., et al., A Sealless Centrifugal Blood Pump with Passive Magnetic and Hydrodynamic Bearings. Artificial Organs, 1999. 23(8): p. 780-784.
3. Gobel, C., et al., Development of the MEDOS/HIA Delta Stream Extracorporeal Rotary Blood Pump. Artificial Organs, 2001. 25(5): p. 358-365.
4. Ohara, Y., et al., Baylor Gyro pump: A completely seal-less centrifugal pump aiming for long-term circulatory support. Artificial Organs, 1993. 17(7): p. 599-604.
5. Jarvik, R. K., System considerations favoring rotary artificial hearts with blood-immersed bearings. Artificial Organs, 1995. 19(7): p. 565-570.
6. Masuzawa, T., et al., Magnetically suspended centrifugal blood pump with an axially levitated motor. Artificial Organs, 2003. 27(7): p. 631-638.
7. Maslen, E., et al., Feedback Control Applications in Artificial Hearts. IEEE Control Systems Magazine, 1998. 18(6): p. 26-34.
8. Akamatsu, T., T. Nakazeki, and H. Itoh, Centrifugal Blood Pump with a Magnetically Suspended Impeller. Artificial Organs, 1992. 16(3): p. 305-308.
9. Golding, L.A. and W. A. Smith, Cleveland clinic rotodynamic pump. The Annals Of Thoracic Surgery, 1996. 61(1): p. 457-462.
10. Watterson, P.A., et al., VentrAssist Hydrodynamically Suspended, Open, Centrifugal Blood Pump. Artificial Organs, 2000. 24(6): p. 475-477.
11. Allaire, P.E., et al., Prototype Continuous Flow Ventricular Assist Device Supported on Magnetic Bearings. Artificial Organs, 1996. 20(6): p. 582-590.
12. Hoshi, H., T. Shinshi, and S. Takatani, Third-generation Blood Pumps With Mechanical Noncontact Magnetic Bearings. Artificial Organs, 2006. 30(5): p. 324-338.
13. Nojiri, C., et al., Development Status of Terumo Implantable Left Ventricular Assist System. Artificial Organs, 2001. 25(5): p. 411-413.
14. Loree, H., et al., The Heartmate III : Design and In Vivo Studies of a Maglev Centrifugal Left Ventricular Assist Device. Artificial Organs, 2001. 25(5): p. 386-391.
15. Bearnson, G. B., et al., HeartQuest Ventricular Assist Device Magnetically Levitated Centrifugal Blood Pump. Artificial Organs, 2006. 30(5): p. 339-346.
16. Mandarino, W.A., et al., Dynamic biventricular response to alterations in preload in patients undergoing left ventricular device implantation. ASAIO J, 1994. 40: p. M295-M298.
17. Nose, Y., et al., Development of a totally implantable biventricular bypass centrifugal blood pump system. Ann Thorac Surg, 1999. 68(2): p. 775-9.
18. Fukamachi, K., et al., Development of a small implantable right ventricular assist device. ASAIO J, 2005. 51(6): p. 730-735.
19. Koen Reesink, et al., Physiologic-insensitive Left Ventricular Assist Predisposes Right-sided Circulatory Failure: A Pilot Simulation and Validation Study. Artificial Organs, 2004. 28(10): p. 933-939.
20. Radovancevic, B., et al., Biventricular support with the Jarvik 2000 axial flow pump: A feasibility study. ASAIO J, 2003. 49(5): p. 604-607.
21. Magliato, K. E., et al., Biventricular support in patients with profound cardiogenic shock: A single center experience. ASAIO J, 2003. 49(4): p. 475-479.
22. Timms, D. L., et al., A complete mock circulation loop for the evaluation of left- right- and bi- ventricular assist devices. Artificial Organs, 2005. 29(7): p. 564–571.
23. Timms, D. L., et al., LVAD Pump Performance And Force Characteristics In A Pulsatile Complete Mock Circulation Loop. Artificial Organs, 2005. 29(7): p. 572-580.
24. Karassik, I. J. and T. McGuire, Centrifugal pumps. 2nd ed. ed. 1998, New York: Chapman & Hall.
25. Japikse, D., W. Marscher, and R. Furst, Centrifugal Pump Design and Performance. 1997, Vermont, USA: Concepts ETI.